THE INFLUENCE OF MASS TRANSPORT PROCESSES ON THE PERFORMANCE OF THE LEAD–ACID CELL

A. D. TURNER and P. T. MOSELEY

Materials Development Division, Building 429, A.E.R.E., Harwell, Nr. Didcot, Oxon. OX11 0RA (U.K.)

(Received March 3, 1980; in revised form April 10, 1982)

Summary

A model of the lead–acid cell is developed in which due regard is given to the influence of mass transport processes operating in the bulk electrolyte as well as within the plates. It is predicted that, at high rates, the capacity of a cell discharged at constant current will be limited by diffusion so that the current density, I, should be related to the discharge time, τ, as $I \propto [\tau]^{-0.5}$. At low rates the capacity will be limited by acid depletion and I will be $\propto [\tau]^{-1.0}$. The model has been tested against published data for commercially available lead/acid batteries and there is good agreement between the predicted and measured I/τ relationships in both the high rate and the low rate regimes. The expressions derived for the capacity of plates discharged in the two regimes also show how the observed positive plate limit on capacity derives from constraints arising out of the two electrode reactions.

Introduction

The useful capacity recoverable from a charged lead–acid cell depends upon a wide range of fundamental parameters which predetermine the response of the cell to selected operating variables such as temperature, discharge current, etc. In order to optimise the performance of the cell, attention must be paid both to the composition of the active material in the electrodes and also to their microstructure. Composition is particularly significant for PbO_2 cathodes because of the widely reported (*e.g.*, [1]) essential requirement that they be prepared electrochemically and the possible link between this requirement and the hydrogen content of the material [2]. Microstructure will represent a key factor in deciding the capacity available at practical rates. Unfortunately both electrode reactions

	Change in Molar Volume
Positive plate: $PbO_2 + 3H_3O^+ + HSO_4^- + 2e^- \rightarrow PbSO_4 + 5H_2O$	+ 91.8%
Negative plate: $H_2O + Pb + HSO_4^- \rightarrow PbSO_4 + H_3O^+ + 2e^-$	+ 167.7%

0378-7753/83/0000-0000/$03.00

are accompanied by very large volume increases of the solid phases, and as discharge proceeds the acid access into the pores of the electrodes becomes progressively restricted. It is clear that the active material is deployed to the best advantage in a microstructure which facilitates contact with the liquid phase reactants at all stages of the reaction. The present paper examines the transport processes involved in maintaining the supply of liquid phase reactants to the site of the current-sustaining reaction, and the controlling influence these processes impose on the accessible capacity of an electrode.

Ions in the electrolyte can move by diffusion, by convection, and by migration under an electric field gradient. The rate of transport by these mechanisms depends on the electrode geometry and porosity, the type of separator in use, the electronic and ionic conductivities of the solid and liquid phases, respectively, and the current/voltage characteristics of the electron transfer reactions at each electrode. Since so many complex and interacting factors are involved in determining the performance characteristics of the lead–acid cell, commercial battery design tends to the empirical, based largely on a manufacturer's experience, and performance has to be assessed by practical tests. Cell capacity at numerous different rates can be collected together by using empirical relationships such as the Peukert equation [3]

$$I^n\tau = \text{constant},$$

where I is the constant discharge current density, τ is the discharge time to some voltage cut-off and n is a constant usually found to take a value between 1.3 and 1.4 [4]. Useful as such equations may be, they give no insight into the factors determining the battery's performance, so any improvement requires expensive and time consuming trials of different empirical design changes. Many of these may prove to have an insignificant effect, or worse, be detrimental to performance. With so many factors interacting to determine the overall behaviour, it is most unlikely that the optimum combination of all the possible variables will be found by trial and error methods, *i.e.*, without quantitative knowledge of the factors limiting performance.

Some years ago it was proposed [5] that porous electrodes, such as are found in the lead–acid cell, could be viewed on a macroscopic scale. It was suggested that the geometric detail of the microporous structure of the electrodes could be disregarded and that variables such as potential and current in the two phases could be successfully treated as continuous functions of time and space. A similar macrohomogeneous model was later applied to the lead–acid battery by Micka and Rousar [6 - 8]. These authors pointed out that the theoretical discharge capacity of the negative plate is higher than that of the positive plate so that cells with equal positive and negative plate areas will normally be positive limited.

The difference in conductivity between the electrolyte and electrode phases, together with the potential dependence of the current density, leads to a non-uniform current distribution through the plate thickness. Since the electrolyte phase has the higher resistivity (even in the fully charged state), the discharge reaction occurs preferentially near the free electrolyte/plate

interface. During discharge the electrolyte concentration becomes depleted and, besides reducing the reaction rate by the law of mass action, this depletion also has the effect of depressing the conductivity of the liquid phase. For high rates of discharge the mass transport of sulphuric acid by diffusion and migration (convection is negligible within the plate pores) is insufficient to replenish that consumed in the cell reaction, so the non-uniformity of current density distribution in the plate is aggravated and the reaction becomes further restricted to a thin surface layer. This is shown by the work of Bode [9] who investigated the spatial distribution of $PbSO_4$ in discharged plates and found that at high discharge rates $PbSO_4$ was concentrated on the outside of the plates while at low rates the distribution was more even.

The macrohomogeneous model has been applied to the lead dioxide electrode by Simonsson [10] who concluded that unless the initial porosity of the electrode was greater than 50%, the utilisation of active material in the plate interior could be curtailed by plugging of the pores by lead sulphate crystals. When the model was used to predict the performance of the positive plate in a battery it was noticed that the decreasing concentration of sulphuric acid in the bulk electrolyte became a significant factor.

In their model of the complete $Pb/H_2SO_4/PbO_2$ cell, Micka and Rousar neglected the effect of changes in electrolyte concentration with distance between the plates (in effect assuming infinitely rapid mass transport of acid from the free electrolyte into the porous plates). In justification of this assumption it was suggested that the electrolyte would become well mixed by natural convection caused by density gradients. While this may be a reasonable view to take of truly free solutions, it seems less reasonable in the presence of fibrous separators and containment bags.

In the present paper the effect of concentration gradients in the electrolyte is explored and the importance of mass transport in determining cell performance is reaffirmed. It is also shown that when bi-logarithmic plots are used to present published data for commercially available batteries, the two principal transport mechanisms manifest themselves in the form of a change of slope.

Principles of the analysis

The elements of a section through one pair of plates in a lead–acid cell are shown schematically in Fig. 1. The charged electrodes consist of porous matrices of electronically conducting active material with their pores filled with electrolyte. Because of the geometric complexity of such structures, it is impractical to consider quantitatively the behaviour of the plates unless a model with a high degree of uniformity is adopted to simplify the mathematics defining the overall parameters such as mass transfer and potential and current distributions. The macrohomogeneous model mentioned above serves this purpose and will form the basis of the present treatment. At any given moment during charge or discharge there will be a large range of reac-

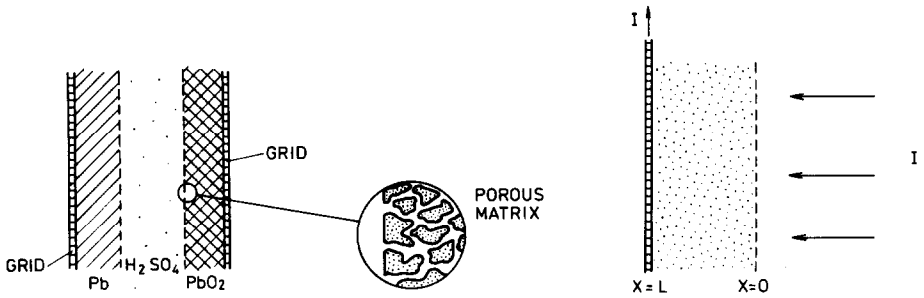

Fig. 1. Schematic representation of a section through a pair of plates in a lead–acid cell.

Fig. 2. Schematic representation of a porous electrode treated as a macrohomogeneous volume with properties varying only in the direction normal to its surface. After Newman and Tobias [5].

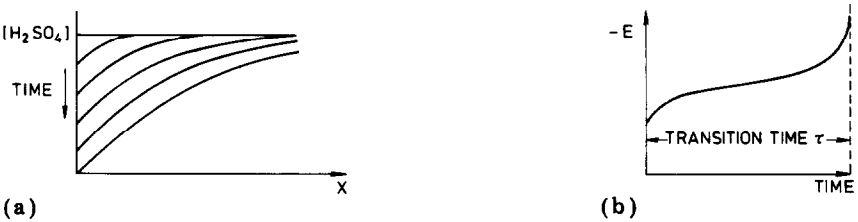

Fig. 3. Constant current discharge at a plane electrode. (a) Schematic representation of the progressive development of the electrolyte concentration profile near the surface; (b) schematic potential–time curve.

tion rates within the pores, the distribution of which will be determined by physical structure, conductivities of electrode and electrolyte and by the parameters that characterize the rate of reaction at the solid/liquid interface — *viz.*, the electrochemical kinetics and the concentration of the electrolyte. This rate distribution (which will change during the course of charge or discharge) directly influences the net power available from a battery. Over the dimensions of a battery plate these microscopic variations can be averaged into continuously varying functions by considering the electrode as a homogeneous region.

The parallel plate configuration, together with the high conductivity current collector used in lead–acid batteries means that the electrode can be considered to be uniform over its face, as shown schematically in Fig. 2. Consequently, quantities such as potentials, current densities, and concentrations vary only with depth into the electrode and not with lateral position. Thus the electrode processes need only be considered in one dimension, *i.e.*, from the current collector, through the active material and into the free electrolyte.

The analysis begins with the consideration of a constant current discharge at a solid plane electrode with a binary electrolyte that is consumed in the electrode reaction to produce an insoluble product that does not occlude electroactive areas of the electrode. Figure 3(a) shows a schematic

representation of the progressive change in electrolyte concentration profile with time near to the electrode surface (at $x = 0$) and Fig. 3(b) shows, again schematically, the potential–time variation for the surface of the plane electrode undergoing constant current discharge. The point of the end of discharge is when the electrolyte concentration at the electrode surface becomes zero (Fig. 3(a)). At this time the potential tends to fall (Fig. 3(b)) due to the increased resistance of the dilute solution. In the model used here, the following assumptions have been made:-

(1) the concentration of acid is small (< 5 molar) compared with the concentration of water (~ 55 molar);

(2) convection in the inter-plate electrolyte is ignored because the fibrous separators and containment bags around the positive electrode restrict movement;

(3) the variation of activity and diffusion coefficients with concentration is also ignored.

Though none of these assumptions is precisely valid in the real battery situation, they give a first order approximation which enables the trends of behaviour to be indicated with reasonable accuracy.

From Appendix 1, the general expression relating the gradient of acid concentration at the electrode surface to the current density is given by:-

$$\frac{|I|}{nF} = \frac{D}{G}\left(\frac{\partial C}{\partial x}\right)_0, \tag{11}$$

where G is a constant with the values of $3 - 2t_+$ and $2t_+ - 1$ for the positive and negative plates, respectively. Equation (11) is a specialized statement of Fick's first law of diffusion.

By considering the mass balance between the acid consumed in the electrode reaction and that transported to the interface by diffusion and migration, Appendix 2 shows that

$$\frac{\partial C}{\partial t} = D\,\frac{\partial^2 C}{\partial x^2} \tag{15}$$

which will be recognised as a statement of Fick's second law of diffusion.

High rate discharge

Figure 3(a) shows schematically how the acid concentration near to one electrode of the one dimensional cell develops with discharge. For the time being the other plate is assumed to be far enough away not to affect the situation and this is a fair assumption for high rate discharge. In Appendix 3 the expression relating discharge time, τ, and current density, I, for discharge at high rates is developed and this is

$$\tau^{1/2} = \frac{FC_\infty\sqrt{\pi D}}{GI} \tag{21}$$

where C_∞ is the initial uniform electrolyte concentration and all other symbols take their earlier meanings.

Low rate discharge

In practice the interplate electrolyte concentration is not infinite in a lead–acid cell so that, on slow discharge, before the end of discharge condition ($C_0(\tau) = 0$) is reached the bulk acid may become depleted to a critical degree. Figure 4 shows a schematic representation of the progressive decrease in acid concentration between a pair of plates as discharge proceeds. In Appendix 4 this model is developed to give an expression relating τ and I for discharge of each plate at low rates:

$$\tau_i = \frac{P_i^2}{D}\left\{\frac{\pi}{4} - G_i\right\} + \frac{2C_\infty P_i F}{I} \tag{26}$$

where P_i represents the distance from each plate to the point of least acid depletion between the plates (see Fig. 4).

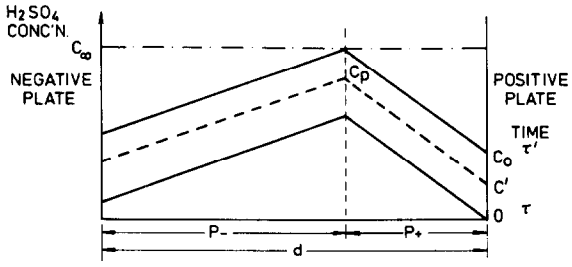

Fig. 4. Distribution of electrolyte concentration between the plates of a lead–acid cell showing depletion at low rate discharge. P_+, P_- represent the distances of the positive and negative plate, respectively, from the acid concentration maximum (C_p).

Influence of the two electrodes considered separately

Considering the capacities of the individual plates as they are allowed to reach the termination condition of $C_0 = 0$:

For high rate discharge eqn. (21) is applied so that for the positive plate capacity

$$I\tau_+ = \frac{C_\infty^2 F^2 \pi D}{G_+^2 I}$$

and for the negative plate

$$I\tau_- = \frac{C_\infty^2 F^2 \pi D}{G_-^2 I} .$$

From the definition of G it is evident that $G_+ > G_-$, *e.g.*, if $t_+ \sim 0.8$ (for 5M H_2SO_4) $G_- \sim 0.6$, $G_+ \sim 1.4$. Therefore

$I\tau_+ < I\tau_-$.

For low rate discharge, applying eqn. (26) gives, for a positive plate, a capacity

$$I\tau_+ = \frac{IP_+^2}{D}\left\{\frac{\pi}{4} - G_+\right\} + 2P_+FC_\infty$$

and for the negative plate

$$I\tau_- = \frac{IP_-^2}{D}\left\{\frac{\pi}{4} - G_-\right\} + 2P_-FC_\infty .$$

Now from eqn. (22) in Appendix (4) it is clear that

$$\frac{P_+}{P_-} = \frac{G_-}{G_+} .$$

So that in the low current limit

$$\frac{I\tau_+}{I\tau_-} = \frac{2P_+FC_\infty}{2P_-FC_\infty} = \frac{G_-}{G_+} .$$

Hence, it is clear that in both these extreme situations the contribution to the capacity from the interplate electrolyte will be positive plate limited for the same geometric plate area. The reason for this dependence originates in the ratio of the factors G_+/G_- which derive from the transport number of the positive ion, and the result is the well known observation that the inefficiency of diffusion and migration transport processes manifests itself first at the positive electrode.

It might be possible to improve energy density somewhat by tailoring the electrode areas to the ratio of active material actually used (*i.e.*, more positive material than negative) but cycle life may then suffer as a consequence of incomplete reversibility of the cell reaction.

Application to real battery data

Expressions have been developed for the dependence of the capacity of a model electrode on the efficiency of transport processes in the electrolyte

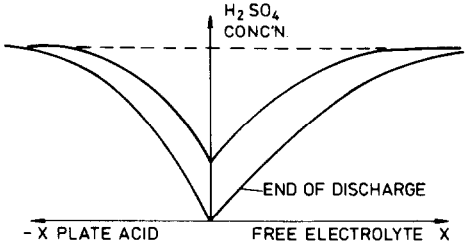

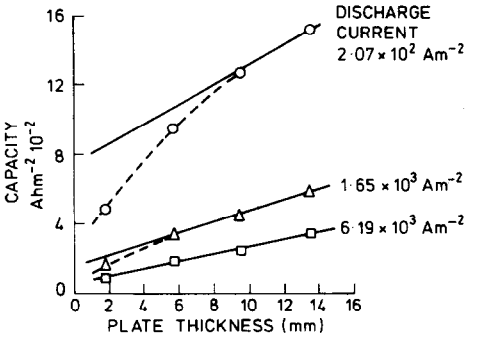

Fig. 5. Schematic representation of the electrolyte profiles in the plate and in the bulk electrolyte during discharge.

Fig. 6. Variation of negative plate constant current discharge capacity with plate thickness. Solid lines represent a fit to the linear part of each curve — originating among the points applying for thick electrodes. The slope of the linear part indicates the change in capacity contributed by acid in the pores of the plate, and the intercept on the capacity axis represents the contribution by acid from the interplate volume. The open points and dashed curves represent measured values taken from ref. 12.

for high and low rate discharges. It is important to test the applicability of these expressions to the real battery situation.

All the current flows from one electrode through the interplate free electrolyte and into the other plate so that it might appear possible to consider both the plate acid, dealt with in earlier treatments [6 - 8], and the free acid, treated here, under the same constant current discharge — especially as they are both limited by the same discharge termination conditions of the acid concentration at the plate/electrolyte interface reaching zero (Fig. 5). Then the effect of the free electrolyte could be allowed for by a simple addition of these contributions.

This hypothesis can be tested since the contribution to the total capacity from the acid contained in the pores is proportional to the plate thickness [12, 13], while the free electrolyte component is independent of this. The variation in capacity with thickness of the negative and positive plates is given in Figs. 6 and 7, respectively, which show data taken from refs. 12 and 13. The majority of the data points — particularly for discharge at the higher rates — fall on straight lines which make a positive intercept on the capacity axis when projected back to zero plate thickness. This positive intercept corresponds to the capacity contributed by the free electrolyte. In the zero plate thickness limit the free electrolyte contribution is no longer used of course and so the real capacity curves (dotted lines) must actually pass through the origin. The departure from the straight line plots is most pronounced for the discharge at lowest current density where there is the greatest free electrolyte contribution to be lost. This pattern of behaviour is exhibited by both plates and thus it can be concluded that the simple addition of the contribution to capacity made by pore electrolyte on the one

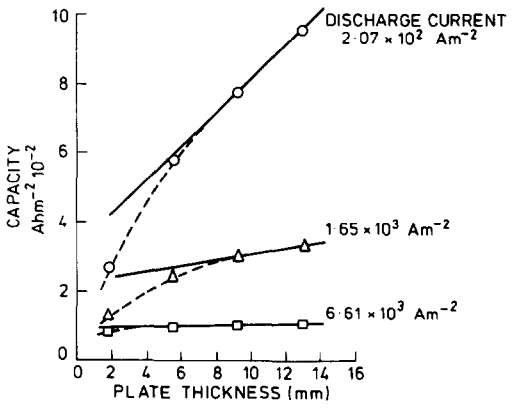

Fig. 7. Variation of positive plate constant current discharge capacity with plate thickness. As in Fig. 6, the solid lines represent a fit to the linear parts of the curves and the dashed curves represent measured values taken from ref. 13.

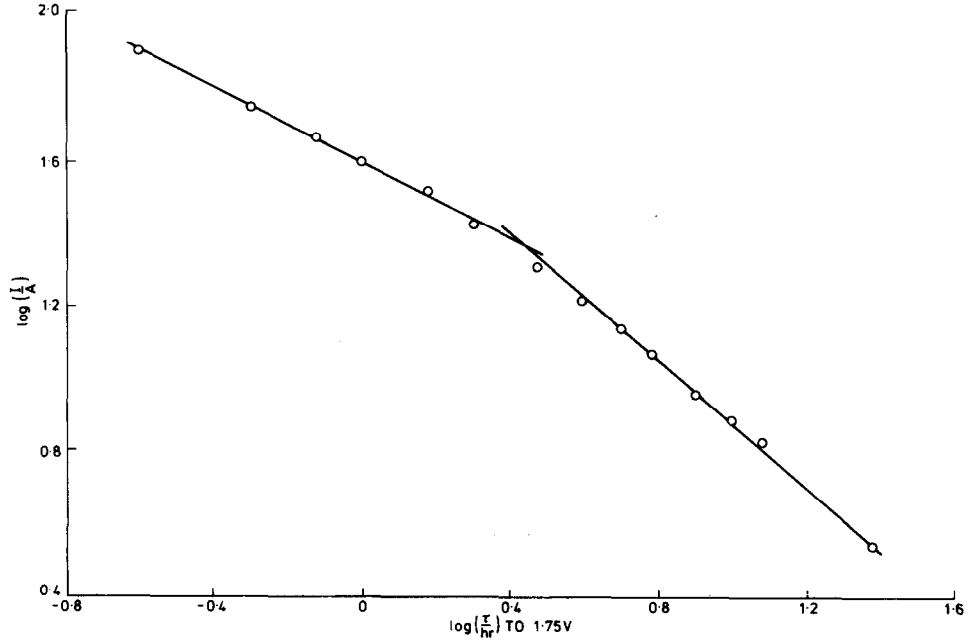

Fig. 8. Bi-logarithmic plot of published data [14] for a lead–acid stationary battery. Specific gravity of electrolyte = 1.215 and temperature = 25 °C. The data for high rates (small values of τ) lie on a line with a slope of −0.5 and the data for low rates lie on a line with a slope of −1.0.

hand and bulk electrolyte on the other is a reasonable approach, particularly for thick electrodes and for high rates of discharge. For a more accurate prediction of cell capacity the computer calculation developed by Micka and Rousar [8] could be extended to allow for concentration variation with distance in the free electrolyte region.

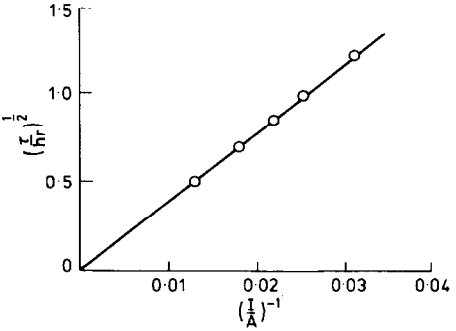

Fig. 9. High rate data from Fig. 8 plotted as $\tau^{0.5}$ against $I^{-1.0}$.

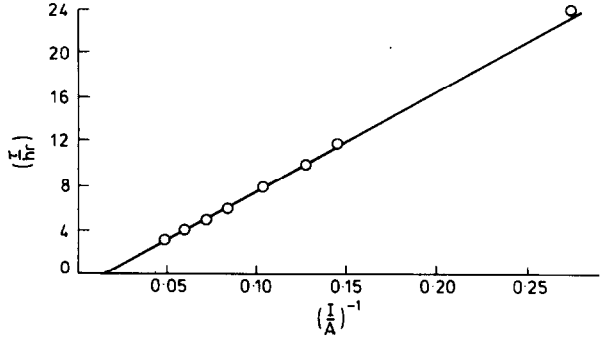

Fig. 10. Low rate data from Fig. 8 plotted as $\tau^{1.0}$ against $I^{-1.0}$.

The expressions for constant current discharge time (eqns. (21) and (26)) indicate that at high rates (short times) the discharge should be governed by $I = K\tau^{-0.5}$ and at low rates by $I = K'\tau^{-1.0}$, where K and K' are constants. When the published data [14] for a lead–acid stationary battery are presented on a bi-logarithmic (Peukert) plot, as in Fig. 8, it is clear that they fit very well to two straight line regions with slopes of approximately -0.5 (at high rates) and -1.0. The agreement with theory is more clearly seen in Figs. 9 and 10 which show the high rate data plotted as $\tau^{1/2}$ against I^{-1} and the low rate data plotted as τ against I^{-1}. Similar good agreement is obtained if the data from ref. 14 for other types of lead–acid batteries are plotted in the same way. The general conformity to this pattern indicates that the plate acid contribution to the capacity shows a switch over in time dependence (from $\tau^{-0.5}$ to $\tau^{-1.0}$) as well as the free electrolyte.

Consideration of eqns. (21) and (26) could also lead to the expectation that capacity should rise with increased acid concentration. Up to a point this will be true, but ultimately the three assumptions made early in the analysis break down and capacity will be limited by pore blockage. Excessively concentrated acid would also cause problems of accelerated grid corrosion.

Discussion

While it is encouraging to find that the expressions for capacity developed here appear to fit the behaviour of commercial batteries, it is pertinent to probe the reasons why the use of the Peukert equation has given single slope plots in other cases. One possible explanation would be that in some cases there might be an overlap of the $\tau^{-0.5}$ and the $\tau^{-1.0}$ regions instead of the rather sharp 'knee' shown in Fig. 8. In a central region where control was shared by diffusion and bulk acid depletion the Peukert slope of around 1.4 could be synthesized out of the two limiting slopes. It is interesting to note that in one careful study [13], where a Peukert plot was obtained which had a mean slope of 1.4, the slope increased to 2.0 at high current density and decreased to 1.03 at low current density.

The method of measuring capacity is also important. The analyses described above are only valid for constant current discharge and would not apply to capacities measured by discharge through a resistor. As the battery voltage started to fall the current would fall and the rate of approach to the end point would decrease.

One further limitation is that of porosity. The present analysis will not be valid for battery discharges which are terminated prematurely owing to pore blockage arising from inadequate initial porosity.

The successful application of the analysis to commercial battery performance indicates that capacity is limited by the transport processes taken into account in the model. Only a change to forced convection of the electrolyte seems likely to contribute substantially to this aspect of lead–acid battery performance. Indeed, a recent report [15] indicates that under conditions of circulating electrolyte, an increase in the capacity of motive power cells can be obtained.

Conclusions

By taking a macroscopic view of the porous electrodes in the lead–acid cell, thereby disregarding the complicated geometric details of their porous structure, it has been possible to treat the mass transport processes in the electrolyte in a quantitative fashion. The analysis predicts that at high rates capacity will be diffusion controlled and the time, τ, of discharge at constant current density, I, should be given by $I = K\tau^{-0.5}$, where K is a constant. At low rates it is predicted that the capacity will be controlled by acid depletion and I will be given by $I = K'\tau^{-1.0}$ where K' is a constant $\neq K$. These two expressions successfully predict the variation of capacity of commercially available lead–acid batteries with discharge rate.

List of symbols

τ	Discharge time to voltage cut-off
τ_+, τ_-	Discharge time for positive and negative plates, respectively

I	Constant discharge current density
n	Number of electrons involved in electrochemical reaction
F	Faraday constant
D	The binary diffusion coefficient = $2D_+D_-/D_+ + D_-$
D_+, D_-	Diffusion coefficient of H_3O^+, HSO_4^-, respectively
C	Electrolyte concentration variable
C_0	Electrolyte concentration at electrode surface
C_∞	Initial uniform electrolyte concentration
x	Distance variable normal to electrode surface
G	Constant = $2t_+ - 1$ for negative plate (G_-), and $3 - 2t_+$ for positive plate (G_+)
t_+, t_-	Transport numbers for H_3O^+, HSO_4^-, respectively.
t	Time variable
C_i	Concentration of species i
V_i	Mean velocity of species i
V_0	Mean velocity of solvent
μ_i	Electrochemical potential of i
R	Universal gas constant
T	Temperature
i	Current density
N_i	Flux of species i
Z_i	Charge on ion i
S_i	Stoichiometry number of species i
μ_e	Chemical potential of the electrolyte
$\beta(S) = \bar{C}$	Laplace transform of concentration with respect to time
S	Laplace transform time variable
σ	Laplace transform distance variable
k^0	Electrochemical rate constant at standard electrode potential
α	Transfer coefficient
η	Potential difference from open circuit voltage
P_+, P_-	Distance from each plate to the point of least acid depletion in the interplate volume

References

1 J. Perkins, *Mater. Sci. Eng., 28* (1977) 167.
2 S. M. Caulder, J. S. Murday and A. C. Simon, *J. Electrochem. Soc., 120* (1973) 1515.
3 W. Peukert, *Elektrotech. Z., 18* (1897) 289.
4 K. Peters, *Chloride Inf. Bull.*, (1975) AM 64.2.
5 J. S. Newman and C. W. Tobias, *J. Electrochem. Soc., 109* (1962) 1183.
6 K. Micka and I. Rousar, *Electrochim. Acta, 18* (1973) 629.
7 K. Micka and I. Rousar, *Electrochim. Acta, 19* (1974) 499.
8 K. Micka and I. Rousar, *Electrochim. Acta, 21* (1976) 599.
9 H. Bode, H. Panesar and E. Voss, *Naturwissenschaften, 55* (1968) 541.
10 D. Simonsson, *J. Appl. Electrochem., 4* (1974) 109.
11 M. Abramowitz and I. Stegun, *Handbook of Mathematical Functions*, Dover, New York, 1976, p. 1020.
12 D. J. Haworth and K. Peters, *EPS Ltd., R & D Dept. Rep. No. 0089/5*, 1971.
13 P. E. Baikie and K. Peters, *EPS Ltd., R & D Dept. Rep. No. 0013/1*, 1970.
14 *The Gould Battery Handbook*, Gould Inc., 1973, p. 271.
15 W. G. Sunu and B. W. Burrows, *J. Electrochem. Soc., 128* (1981) 1405.

Appendix 1

The general expression relating current density to the electrolyte concentration gradient at the electrode surface

The equation for the flux of component i in concentrated solution can be written:

$$N_i = C_i V_i = C_i V_0 - \frac{D_i C_i}{RT} \frac{\partial \mu_i}{\partial x}$$

where the term $C_i V_0$ represents the contribution made by convection, and the term involving the electrochemical potential, μ_i, covers the effects of both ion migration and diffusion.

In the case of the plates in a lead–acid battery surrounded by separators and containment bags the convection term can be ignored and the equation reduces to

$$N_i = -\frac{D_i C_i}{RT} \frac{\partial \mu_i}{\partial x}. \tag{1}$$

For acid of the strength normally used in batteries the equilibrium

$$H_2SO_4 \rightleftarrows H^+ + HSO_4^-$$

lies well to the right and we can safely write

$$C = C_+ = C_-. \tag{2}$$

The positive plate electrode reaction is, effectively,

$$PbO_2 + 3H^+ + HSO_4^- + 2e^- \rightarrow PbSO_4 \downarrow + 2H_2O.$$

The flux of HSO_4^- will be designated as N_- and the flux of H^+ as N_+ so that, arising from mass balance at the surface of the electrode

$$\sum_i Z_i N_i = \frac{i}{nF} \tag{3}$$

and

$$\frac{\partial C_i}{\partial t} = \frac{-\partial N_i}{\partial x} - \delta_i \tag{4}$$

where

$$\delta_i = \frac{S_i}{nF}\frac{\partial i}{\partial x}$$

and S_i is the stoichiometry number for species i.

From eqn. (2)

$$\frac{\partial C_+}{\partial t} = \frac{\partial C}{\partial t} = \frac{-\partial N_+}{\partial x} + \frac{3}{2F}\frac{\partial i}{\partial x} \text{ since } n = -2$$

and

$$\frac{\partial C_-}{\partial t} = \frac{\partial C}{\partial t} = \frac{-\partial N_-}{\partial x} + \frac{1}{2F}\frac{\partial i}{\partial x}$$

by subtraction

$$\frac{\partial N_+}{\partial x} - \frac{\partial N_-}{\partial x} = \frac{1}{F}\frac{\partial i}{\partial x}$$

which, by back substitution gives

$$\frac{\partial C}{\partial t} = \frac{1}{2}\frac{\partial N_+}{\partial x} - \frac{3}{2}\frac{\partial N_-}{\partial x}$$

so that, in a pseudo steady state where $\partial C/\partial t = 0$

$$N_+ = 3N_-. \tag{5}$$

Now the chemical potential of the electrolyte due to its electroneutrality is given by

$$\mu_e = \nu_+\mu_+ + \nu_-\mu_- \tag{6}$$

so that

$$\frac{\partial \mu_e}{\partial x} = \frac{\partial \mu_+}{\partial x} + \frac{\partial \mu_-}{\partial x} = RT\frac{\partial}{\partial x}(\ln a_\pm^\nu)$$

where $\nu = \nu_+ + \nu_-$.

Ignoring the variation of activity coefficient with concentration

$$\frac{\partial \mu_e}{\partial x} = RT\frac{\partial}{\partial x}\ln C^\nu = \frac{\nu RT}{C}\frac{\partial C}{\partial x}. \tag{7}$$

From eqns. (1) and (5)

$$D_+\frac{\partial \mu_+}{\partial x} = 3D_-\frac{\partial \mu_-}{\partial x}. \tag{8}$$

Now the total current is given by the sum of the fluxes

$$\frac{I}{F} = N_+ - N_- = \frac{-D_+C_+}{RT}\frac{\partial\mu_+}{\partial x} + \frac{D_-C_-}{RT}\frac{\partial\mu_-}{\partial x} \text{ (from eqn. (1))}$$

which, combined with eqns. (2) and (8), becomes

$$\frac{I}{F} = \frac{-3D_-C}{RT}\frac{\partial\mu_-}{\partial x} + \frac{D_-C}{RT}\frac{\partial\mu_-}{\partial x} = \frac{-2D_-C}{RT}\frac{\partial\mu_-}{\partial x}.$$

Now combining eqns. (6) and (8) gives

$$\frac{D_-\partial\mu_-}{\partial x} = \frac{D_-D_+}{(3D_- + D_+)}\frac{\partial\mu_e}{\partial x}$$

so that

$$\frac{I}{F} = \frac{-2D_-D_+C}{(3D_- + D_+)RT}\frac{\partial\mu_e}{\partial x}.$$

Taking account of eqn. (7),

$$\frac{C\partial\mu_e}{\partial x} = 2RT\frac{\partial C}{\partial x}$$

gives

$$\frac{I}{F} = \frac{-4D_-D_+}{(3D_- + D_+)} \cdot \frac{\partial C}{\partial x}.$$

Now writing D as the binary diffusion coefficient

$$\frac{2D_+D_-}{D_+ + D_-}$$

$$\frac{I}{F} = \frac{-2D(D_+ + D_-)}{3D_- + D_+} \cdot \frac{\partial C}{\partial x}$$

and since the positive ion transport number,

$t_+ = D_+/(D_+ + D_-)$

$$\frac{I}{2F} = \frac{-D}{(3 - 2t_+)} \cdot \frac{\partial C}{\partial x}$$

or

$$\frac{|I|}{nF} = \frac{D}{(3-2t_+)} \cdot \frac{\partial C}{\partial x}, \qquad \text{since } n = 2. \tag{9}$$

Similarly for the negative plate reaction

$$Pb + HSO_4^- \rightarrow PbSO_4\downarrow + H^+ + 2e^-$$

the mass balance at the electrode surface gives

$$\frac{\partial C_+}{\partial t} = \frac{\partial C}{\partial t} = \frac{-\partial N_+}{\partial x} + \frac{1}{2F}\frac{\partial i}{\partial x} \qquad \text{since } S_+ = -1 \text{ and } n = 2$$

and

$$\frac{\partial C_-}{\partial t} = \frac{\partial C}{\partial t} = \frac{-\partial N_-}{\partial x} - \frac{1}{2F}\frac{\partial i}{\partial x} \qquad \text{since } S_- = 1.$$

Hence

$$N_+ = -N_- \text{ and } D_+\frac{\partial \mu_+}{\partial x} = D_-\frac{\partial \mu_-}{\partial x}.$$

Combining positive and negative ion fluxes

$$\frac{I}{F} = N_+ - N_- = \frac{-D_+C}{RT}\frac{\partial \mu_+}{\partial x} + \frac{D_-C}{RT}\frac{\partial \mu_-}{\partial x}$$

$$= \frac{-2D_+C}{RT}\frac{\partial \mu_+}{\partial x}.$$

Now in this case

$$\frac{\partial \mu_e}{\partial x} = \frac{\partial \mu_+}{\partial x} = \frac{\partial \mu_-}{\partial x}$$

$$= \frac{\partial \mu_+}{\partial x}\left(\frac{D_- - D_+}{D_-}\right).$$

Hence

$$\frac{I}{F} = \frac{-2D_+D_-}{D_- - D_+} \cdot \frac{C}{RT} \cdot \frac{\partial \mu_e}{\partial x}$$

and as before

$$\frac{C\partial\mu_e}{\partial x} = 2RT\frac{\partial C}{\partial x}$$

so that

$$\frac{I}{F} = \frac{-4D_+D_-}{(D_- - D_+)}\frac{\partial C}{\partial x}$$

$$= \frac{-2(D_- + D_+)}{(D_- - D_+)}\frac{D\partial C}{\partial x} = \frac{2D}{(1-2t_+)}\frac{\partial C}{\partial x}$$

and

$$\frac{|I|}{nF} = \frac{D}{(2t_+ - 1)} \cdot \frac{\partial C}{\partial x}. \tag{10}$$

A general expression of eqns. (9) and (10) would be

$$\frac{|I|}{nF} = \frac{D}{G} \cdot \left(\frac{\partial C}{\partial x}\right)_0 \tag{11}$$

where G is a constant describing the effect of the electric field on transport and is numerically equal to $3 - 2t_+$ for the positive plate and $2t_+ - 1$ for the negative plate. The subscript 0 signifies that the term represents the concentration gradient at the electrode surface.

Appendix 2

Transport of species in the bulk of the electrolyte

In the bulk of the solution no reaction is taking place so that eqn. (4) (Appendix 1) becomes

$$\frac{\partial C_i}{\partial t} = \frac{-\partial N_i}{\partial x} = \frac{D_i}{RT}\frac{\partial}{\partial x}\left(C_i\frac{\partial\mu_i}{\partial x}\right).$$

Since $\nu_- = \nu_+ = 1$ and $C = C_+ = C_-$

$$\frac{\partial C}{\partial t} = \frac{D_+}{RT}\cdot\frac{\partial}{\partial x}\left(\frac{C\partial\mu_+}{\partial x}\right) = \frac{D_-}{RT}\frac{\partial}{\partial x}\left(\frac{C\partial\mu_-}{\partial x}\right). \tag{12}$$

Thus

$$\frac{\partial}{\partial x}\left(D_+ \frac{C\partial\mu_+}{\partial x}\right) = \frac{\partial}{\partial x}\left(D_- \frac{C\partial\mu_-}{\partial x}\right)$$

and since

$$\frac{\partial}{\partial x}\left(\frac{C\partial\mu_e}{\partial x}\right) = \frac{\partial}{\partial x}\left(\frac{C\partial\mu_+}{\partial x}\right) + \frac{\partial}{\partial x}\left(\frac{C\partial\mu_-}{\partial x}\right)$$

therefore

$$\frac{\partial}{\partial x}\left(\frac{C\partial\mu_+}{\partial x}\right) = \frac{D_-}{D_+ + D_-}\frac{\partial}{\partial x}\left(\frac{C\partial\mu_e}{\partial x}\right). \tag{13}$$

From eqn. (7) in Appendix 1 with $\nu = 2$

$$\frac{C\partial\mu_e}{\partial x} = 2RT\frac{\partial C}{\partial x}$$

so that

$$\frac{\partial}{\partial x}\left(\frac{C\partial\mu_e}{\partial x}\right) = 2RT\frac{\partial^2 C}{\partial x^2} \tag{14}$$

and, substituting eqns. (13) and (14) in eqn. (12) gives

$$\frac{\partial C}{\partial t} = \frac{D_+}{RT}\cdot\frac{D_-}{(D_+ + D_-)}\cdot 2RT\frac{\partial^2 C}{\partial x^2}$$

$$= D\frac{\partial^2 C}{\partial x^2}. \tag{15}$$

Appendix 3

High rate discharge

The one dimensional half-cell is represented as in Fig. 3(a) with $x = 0$ being the electrode plate surface. The binary electrolyte is transported towards the electrode where it is consumed in the electrode reaction according to eqn. (15):

$$\frac{\partial C}{\partial t} = D\frac{\partial^2 C}{\partial x^2}$$

replacing $y = x/\sqrt{D}$ (16)

then

$$\frac{\partial C}{\partial t} = \frac{\partial^2 C}{\partial y^2}.$$

Taking the Laplace transform with respect to time (S)

$$\mathcal{L}\frac{\partial C}{\partial t} = \mathcal{L}\frac{\partial^2 C}{\partial y^2}$$

for which solutions have been tabulated [11]

$$\mathcal{L}\frac{\partial C}{\partial t} = \int_0^\infty \frac{\partial C}{\partial t}\exp(-st)\,dt = S\int_0^\infty \exp(-st)\,C dt - C_{t=0}$$

$$= S\bar{C} - C_\infty \ (C_\infty \text{ is the bulk concentration at } t = 0).$$

Thus

$$S\bar{C} - C_\infty = \mathcal{L}\frac{\partial^2 C}{\partial y^2} = \frac{\partial^2 \bar{C}}{\partial y^2}.$$

Let $\bar{C} = \beta$

then

$$S\beta - C_\infty = \frac{\partial^2 \bar{C}}{\partial y^2} = \frac{\partial^2 \beta}{\partial y^2}$$

and, taking a second set of Laplace transforms, this time with respect to distance, σ,

$$S\int_0^\infty \exp(-\sigma y)\,\beta dy - C_\infty \int_0^\infty \exp(-\sigma y)\,dy$$

$$= S\bar{\beta} - \frac{C_\infty}{\sigma} = \sigma^2\bar{\beta} - \sigma\beta_0 - \beta_0' \qquad (17)$$

where σ is the transform distance variable and the solution is again obtained from tables [11].

Now $\beta_0' = \mathcal{L}_t(dC/dy)_0$ and for constant current discharge $(dC/dy)_0$ is not a function of time, so if $(dC/dy)_0$ is set equal to j (18) then

$$\mathcal{L}_t j = \frac{j}{S}.$$

Now eqn. (17) becomes

$$S\bar{\beta} - \frac{C_\infty}{\sigma} = \sigma^2\bar{\beta} - \sigma\beta_0 - \frac{j}{S}$$

and

$$\bar{\beta} = \frac{\sigma\beta_0}{(\sigma^2 - S)} + \frac{j}{S(\sigma^2 - S)} - \frac{C_\infty}{\sigma(\sigma^2 - S)}.$$

Inverting the distance transform (11)

$$\beta = \beta_0 \cosh(\sqrt{S}\, y) + \frac{j}{S\sqrt{S}} \sinh(\sqrt{S}y) + \frac{C_\infty}{S} - \frac{C_\infty}{S}\cosh(\sqrt{S}y).$$

However, as concentrations are finite everywhere in space, β does not tend to ∞ as y gets larger, so that the coefficients of e^y in the cosh and sinh terms must sum to zero:-

$$\beta_0 + \frac{j}{S\sqrt{S}} - \frac{C_\infty}{S} = 0.$$

Now inverting the time transform (11) gives

$$C_0(t) = C_\infty - 2j\sqrt{\frac{t}{\pi}}. \tag{19}$$

If the battery is supplying a sufficient current (*i.e.*, a practical current) then there is enough polarization to express the current/interfacial potential relationship as

$$\frac{I}{2F} = k^0 C_0 \exp(-\alpha\eta F/RT)$$

where k^0 is the electrochemical rate constant at $\eta = 0$ (η is the potential difference from the open circuit voltage).

C_0 from the above gives

$$\frac{I}{2F} = k^0\left\{C_\infty - \frac{2j\sqrt{t}}{\sqrt{\pi}}\right\}\exp(-\alpha\eta F/RT).$$

As I is constant, there will come a time t when the value inside the brackets approaches zero, and thus the potential starts to approach $-\infty$ (see Fig. 3(b)). This will happen when $C(0,\tau) = 0$ or $C_\infty = 2j\sqrt{\tau}/\sqrt{\pi}$.

If current continues to pass after this point, other electrode processes will have to take over and severe damage will be done. Thus, in practice, the termination of discharge voltage (when $t = \tau$) is defined as the potential when the voltage/time trace starts to fall rapidly.

As $j = GI/2F\sqrt{D}$ from eqns. (11), (16) and (18), (20)

eqn. (19) gives

$$C_\infty = \frac{2GI}{2F}\frac{\sqrt{\tau}}{\sqrt{\pi D}} - \text{that is } \tau^{1/2} = \frac{FC_\infty\sqrt{\pi D}}{GI} \tag{21}$$

or $\tau^{1/2} = H/I$ (where H is a constant).

Appendix 4

Low rate discharge

The mass of electrolyte in the cell is not infinite so that, on slow discharge, before the condition of end of discharge $C(0, \tau) = 0$ is reached the bulk acid concentration may have been depleted.

Considering a box between the positive and negative plates of width $P(= P_+ + P_-)$ as shown in Fig. 4 and making use of the simple approximation

$$\frac{GI}{nF} = D\left(\frac{\partial C}{\partial x}\right)_0 \text{ (eqn. (11))} = D\frac{(C_p - C')}{P} = D\frac{(C_\infty - C_0)}{P} \tag{22}$$

for a constant current discharge.

On rearrangement

$$\frac{GIP}{nFD} + C' = C_p.$$

At time τ' there is a change from semi-infinite diffusion to a depletion/diffusion mode. At this point in time, the total number of moles of acid left in the box is $(C_\infty + C_0)P/2$. After this time, the number of moles consumed in time δt is $I\delta t/nF$.

Thus we can write the total number of moles present in the box at $t > \tau'$

$$(C_\infty + C_0)\frac{P}{2} - \int_{\tau'}^{t}\frac{I\mathrm{d}t}{nF} = (C_p + C')\frac{P}{2}.$$

Rearranging and substituting for C_p from above,

$$2C' + \frac{GIP}{nFD} = C_\infty + C_0 - \frac{2}{P}\frac{(t-\tau')I}{nF}.$$

When $t = \tau$, C' has become zero — the end of discharge.

Writing $\Delta\tau = \tau - \tau'$

$$\frac{GIP}{nFD} = C_\infty + C_0 - \frac{2\Delta\tau I}{PnF}.$$

From eqns. (19) and (20) we can find the value of C_0 and τ' when we switch over from semi-infinite diffusion to the depletion case

$$C_0(\tau') = C_\infty - \frac{GI\sqrt{\tau'}}{\sqrt{\pi DF}}. \tag{23}$$

Thus

$$\frac{GIP}{nFD} = 2C_\infty - \frac{GI\sqrt{\tau'}}{\sqrt{\pi DF}} - \frac{2\Delta\tau I}{PnF}. \tag{24}$$

Now as from eqn. (22)

$$D\frac{(C_\infty - C_0)}{P} = \frac{GI}{nF}$$

and from eqn. (23)

$$\frac{D(C_\infty - C_0)}{P} = \frac{DGI\sqrt{\tau'}}{FP\sqrt{\pi D}},$$

therefore

$$\frac{GI\sqrt{\tau'}}{F\sqrt{\pi D}} = \frac{GIP}{2DF} \tag{25}$$

so

$$\tau = \frac{P^2\pi}{4D}.$$

From eqns. (24) and (25) since $n = 2$

$$\frac{GIP}{2DF} = C_\infty - \frac{\Delta\tau I}{2PF} \quad \text{and therefore} \quad \Delta\tau = \frac{2PF}{I}\left\{C_\infty - \frac{GIP}{2DF}\right\}.$$

Now, as $\tau = \tau' + \Delta\tau$

$$\tau = \frac{P^2\pi}{4D} + \frac{2PF}{I}\left\{C_\infty - \frac{GIP}{2DF}\right\} = \frac{P^2}{D}\left\{\frac{\pi}{4} - G\right\} + 2\frac{C_\infty PF}{I}. \tag{26}$$